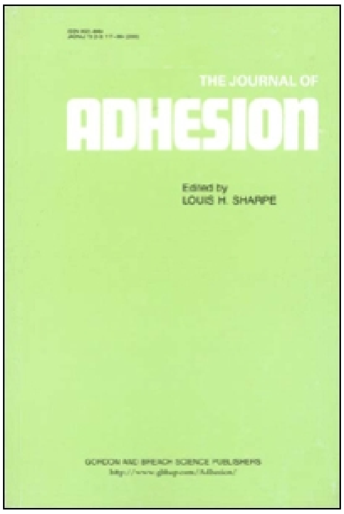

The Journal of Adhesion
Publication details, including instructions for authors and subscription information:
http://www.informaworld.com/smpp/title~content=t713453635

Nuclear Magnetic Resonance Images (NMRI) of *In Situ* Epoxy Curing Behavior in Anodized and Untreated Aluminum Bonded Joints

F. Fondeur[a]; J. L. Koenig[a]
[a] Department of Macromolecular Science, Case Western Reserve University, Cleveland, Ohio, USA

To cite this Article Fondeur, F. and Koenig, J. L.(1993) 'Nuclear Magnetic Resonance Images (NMRI) of *In Situ* Epoxy Curing Behavior in Anodized and Untreated Aluminum Bonded Joints', The Journal of Adhesion, 43: 4, 289 — 307
To link to this Article: DOI: 10.1080/00218469308026608
URL: http://dx.doi.org/10.1080/00218469308026608

J. Adhesion, 1993, Vol. 43, pp. 289–308
Reprints available directly from the publisher
Photocopying permitted by license only

Printed in the United States of America

Nuclear Magnetic Resonance Images (NMRI) of *In Situ* Epoxy Curing Behavior in Anodized and Untreated Aluminum Bonded Joints

F. FONDEUR and J. L. KOENIG*

Department of Macromolecular Science, Case Western Reserve University,
Cleveland, Ohio 44106-7202, USA

(Received August 26, 1992; in final form August 5, 1993)

Nuclear Magnetic Resonance Imaging (NMRI) was used to analyze the curing behavior of epoxy adhesives in the presence of anodized and chemically-treated aluminum surfaces. The proton images of epoxy between untreated Al plates are characterized by large amounts of inhomogeneities (fine texture of high and low mobility regions) finely distributed throughout the sample. Large uncured domains of epoxy were found aggregated and near the center of the bonded adhesive sample. Dispersion of uncured material during curing is observed through redistribution of intensity in the images with cure time. The anodized aluminum-epoxy samples, on the other hand, showed very small contrast and coarse texture images. However, the onset of curing was clearly shown with increases in contrast and texture. Large amounts of uncured material were seen near the anodized surfaces. This effect was more pronounced in the chromic acid anodized aluminum samples (CAA).

KEY WORDS NMRI; interface; epoxy; anodize; aluminum; imaging; image analysis; chromic acid anodizing; sulfuric acid anodizing; chemically-treated aluminum; Iridite-14®; uncured epoxy domains.

INTRODUCTION

The curing behavior of adhesive systems has been studied extensively by a number of surface techniques and considerable insight into the interfacial reactions between epoxy and metal substrates has been obtained.[1–4] However, all of these techniques are limited to thin films deposited on the metal surface and to date no technique has allowed the study of the *in situ* curing of, *e.g.*, an epoxy adhesive between metal substrates. NMR imaging (NMRI) can reveal the spatial aspects of cured adhesives and, in this study, we report proton images of the epoxy cured between Al plates which have been anodized and chemically treated.

---

*Corresponding author.

EXPERIMENTAL

Preparation of Substrate

Aluminum (2024-T3) coupons (0.5 × 0.5 inch) (12.7 × 12.7 mm) were mechanically polished to 3 μm roughness and then degreased with 2-butanone. The coupons were then sent to a plating company to be anodized in sulfuric acid solutions (SAA) and chromic acid solutions (CAA) according to Mil-A8625-E specifications as follows:

TABLE I

	Type II		Type I
Sulfuric Acid	20 wt%	Chromic Acid	5 wt%
Water	80 wt%		95 wt%
volts	18 volts		40 volts
current	23 Amps/ft^2 (0.025 Amp/cm^2)		1.5 Amps/ft^2 (0.0016 Amps/cm^2)
temperature	20°C		40°C
time	60 Min.		30 Min.
thickness	34 μm		19 μm

The coupons were also etched in a solution of cyano-chromic acid complex (Iridite I-14®). Samples were kept in a desiccator under vacuum after treatment.

Adhesive

The epoxy resin used was a bisphenol-A type (Epon 828®, Shell) and the curing agent was dicyandiamide (dicy) at a concentration of 7 phr. Durion® (Dow Chemical) was used at a concentration of 1 phr as an accelerator. The structures of the materials are given in Figure 1.

Bonded Samples

Aluminum coupons (1.2 cm × 1.2 cm) were used to make joints with 0.84 cm^2 adhesive area. The 0.5 mm joint thickness was obtained by using Teflon® shims. Samples were cured for a period of 12 minutes at 175°C and then imaged.

NMRI

The NMR images were obtained on a Bruker MSL 300 FT-NMR spectrometer at a proton frequency of 300 megahertz. The spectrometer was equipped with a micro-imaging accessory and a sample probe with a diameter of 15 mm.

The experiment was a typical Carr-Purcell[7,8] spin-echo pulse sequence with a selective 90-degree pulse and a non-selective 180-degree pulse with CYCLOPS phasing. Typical duration times for the 90-degree pulse were 1 msec and for the 180-degree pulse 113 msec. The echo time was 12 msec (this is the fastest switching time with the instrument) and the corresponding repetition time was one second.

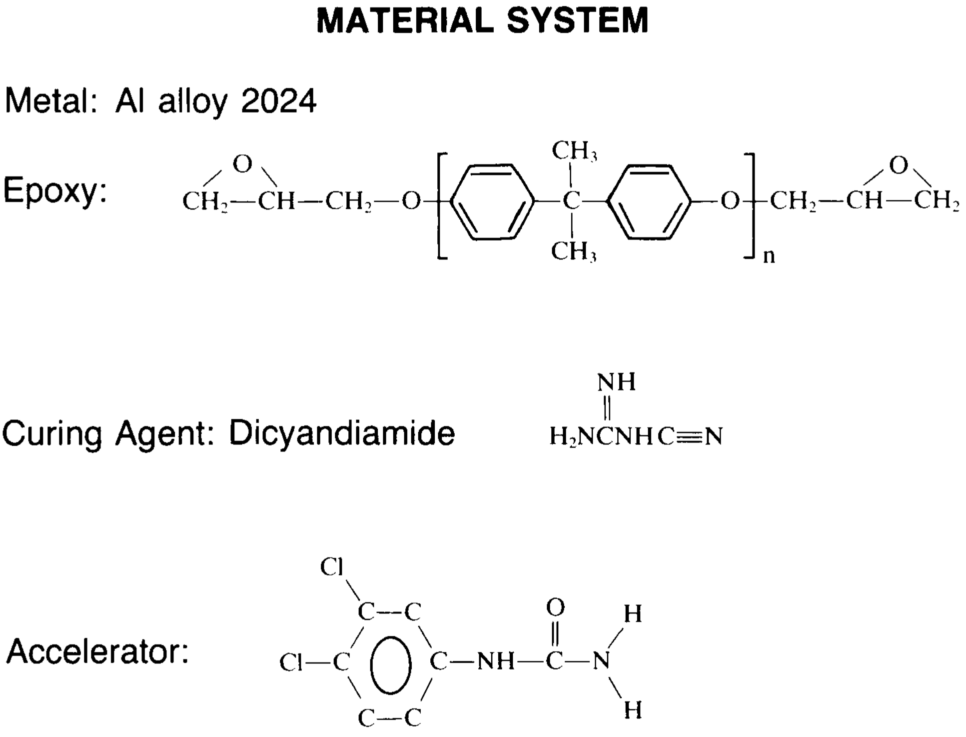

FIGURE 1 Materials used in this work.

A non-selective 90-degree pulse was used for the proton shadowgram. Magnetic field gradients were 9–10 Gauss/cm in the in-plane space and 2–3 Gauss/cm in the Z-direction. The protons of the methyl unit in the gem dimethyl were imaged.

Images of aluminum plates immersed in distilled water showed image distortion at the corners of the aluminum plates but not at the edges. The distortion at the corners was characterized by a highly intense signal (red color) but the basic shapes of the plates was not distorted. Furthermore, when the aluminum plates were placed along the XZ-direction, the signal distortions at the corners of the plates were minimized because the Y-gradient field is zero. Thus, all of the samples were placed in the XZ-direction where the Z-direction is the direction of the static magnetic field. Further, when the HNMR spectrum of the pure epoxy resin between aluminum plates was obtained using the imaging accessories with the gradient field off, the linewidth of the resulting proton peak was similar to the linewidth of the resulting proton peak for the epoxy resin in a glass test tube.

Proton images of the epoxy resin between treated and untreated aluminum plates showed no distortion, agreeing with results published earlier.[10] The contrast in the images is due to differences in spatial T_2 originating from the different degrees of cure in the sample. Thus, as the sample cures the T_2 values become smaller and the time and spatial variation of these values is characteristic of the epoxy curing behavior. Inhomogeneities due to RF field-metal interactions were minor in this experiment and they should not change in time. Since mechanical mixing of epoxy with dicyandiamide always leads to heterogeneous mixtures, mixing was done in the same way and to the same extent for all the samples. The intensity at a given pixel reflects the cured state of the pixel due to line broadening. In our case, at 0.2 hours of cure the line width was 60 Hertz (pixel size approximately 0.0016 cm^2), at 0.6 hours it was 172 Hertz and at 0.8 hours it was 281 Hertz. These widths compare with the 244 Hertz/pixel resolution in the X-direction. Further, the intensity at a given pixel is the result of time averaging (17 minutes) the curing process at that pixel. Finally, the effects of the chemical shift due to other nuclei add shadows to the intensity in the images. We feel that the most important of the above effects is the line broadening due to the curing process. The result of this effect on the images is to homogenize them (that is, to make the cured domains look bigger than they really are). Nevertheless, the texture obtained early in the curing process is a spated (*i.e.*, spattered) fingerprint of the epoxy curing behavior.

RESULTS

Cross Sectional View of the Al/Epoxy Samples

A set of four NMRI images was obtained from each of the chemically-treated and untreated aluminum samples. A typical set of images is shown in Figure 2 for the CAA-treated sample. In the images, the red corresponds to high mobility and blue to low mobility. The 0.2 hour-cured image was not processed as indicated by the few red dots in the image (these few red areas are due to a spike in the middle of the image that was electronically removed). The degree of cure is reflected by the small decrease in total signal.

In order to view the spatial distribution of the curing domains, enhanced images (2.5x) of the treated and untreated samples are shown in Figures 3–5. Figure 3 shows a segmented image of the uncured and cured domains in the CAA-epoxy sample. Segmentation was set from 230 to 255 gray scale for the high mobility domains (255 corresponds to the red color which is the signal obtained for the uncured adhesive) and from 200 to 1 gray scale for the low mobility domains. This segmentation allows one to visualize those domains that cure faster and their segregation tendencies. It clearly shows that most of the uncured epoxy (shown in red) is at the interface of the sample even though some uncured epoxy is not at the interface.

A contrasting behavior is seen for the untreated aluminum-epoxy sample cured at 175°C for 0.6 hours (see Figure 4). The figure shows the uncured epoxy segregated at the center of the sample and away from the interface.

In the case of the chemically-treated aluminum (Iridite®)-epoxy sample, the image at 0.6 hours of cure (see Figure 5) shows a more homogeneous cure of the resin and there are few domains that are uncured at this curing time. The colors in the images are referenced to the uncured adhesive.

Thus, the uncured epoxy in epoxy adhesive-anodized aluminum joints is at the surface while for untreated aluminum joints it is away from the surface (center of the bond) as shown simply in Figure 6 (dark regions correspond to uncured regions).

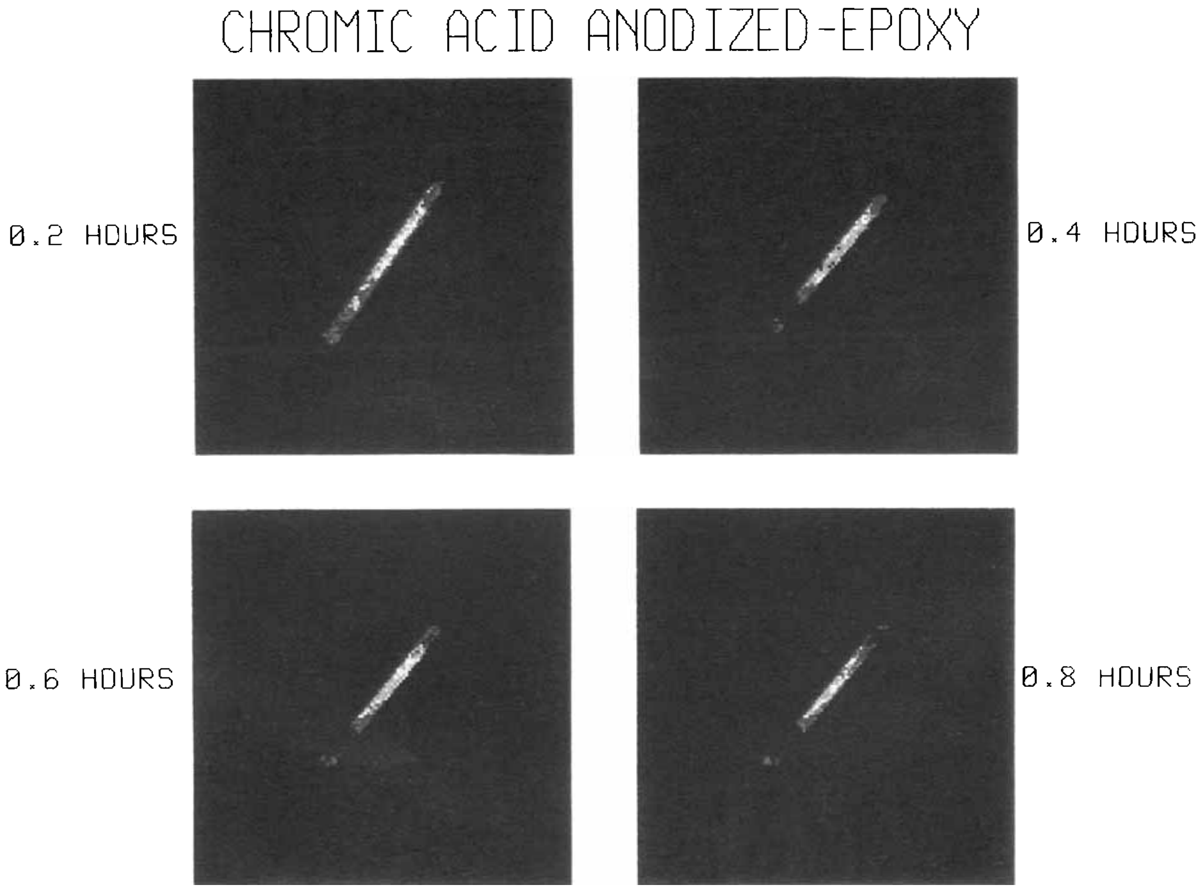

FIGURE 2 Cross-sectional NMRI images of a CAA-epoxy sample as a function of cure time. The red color areas are uncured domains and the green areas are cured domains. **See Color Plate I.**

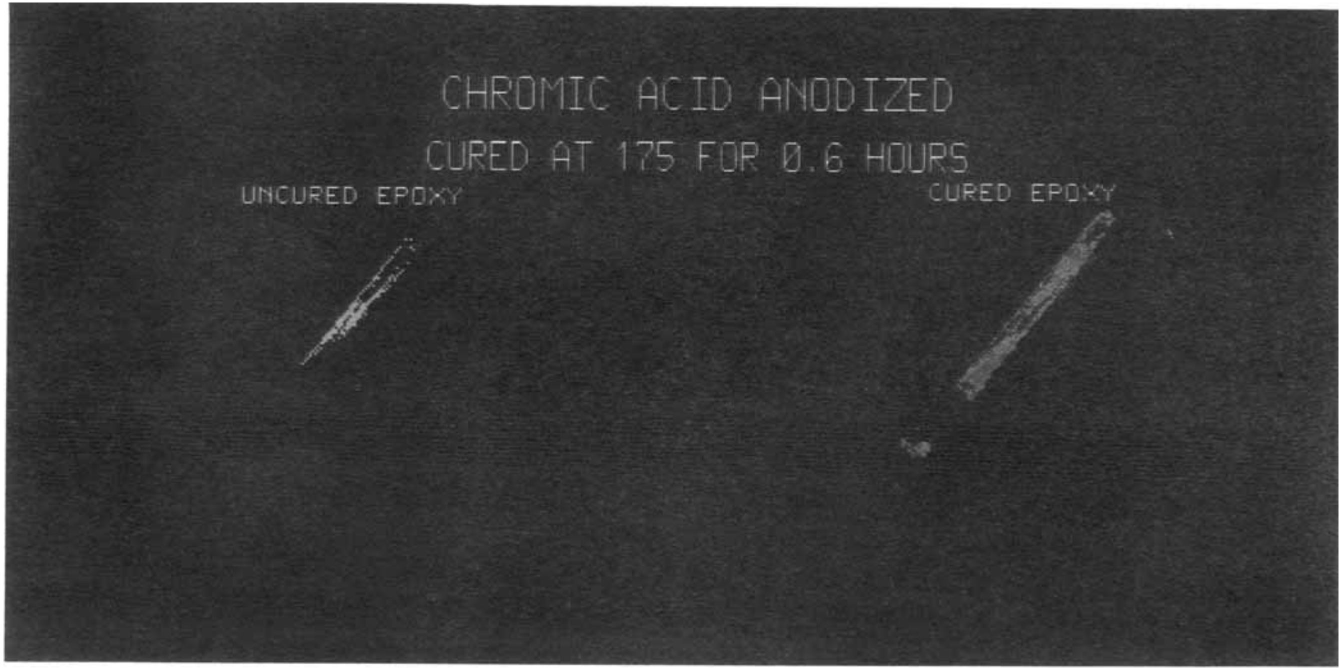

FIGURE 3 Cross-sectional NMRI images of a CAA-epoxy sample segmented into uncured and cured regions. The red area corresponds to uncured epoxy and the green area corresponds to cured epoxy. The image has been magnified 2.5 times. See Color Plate II.

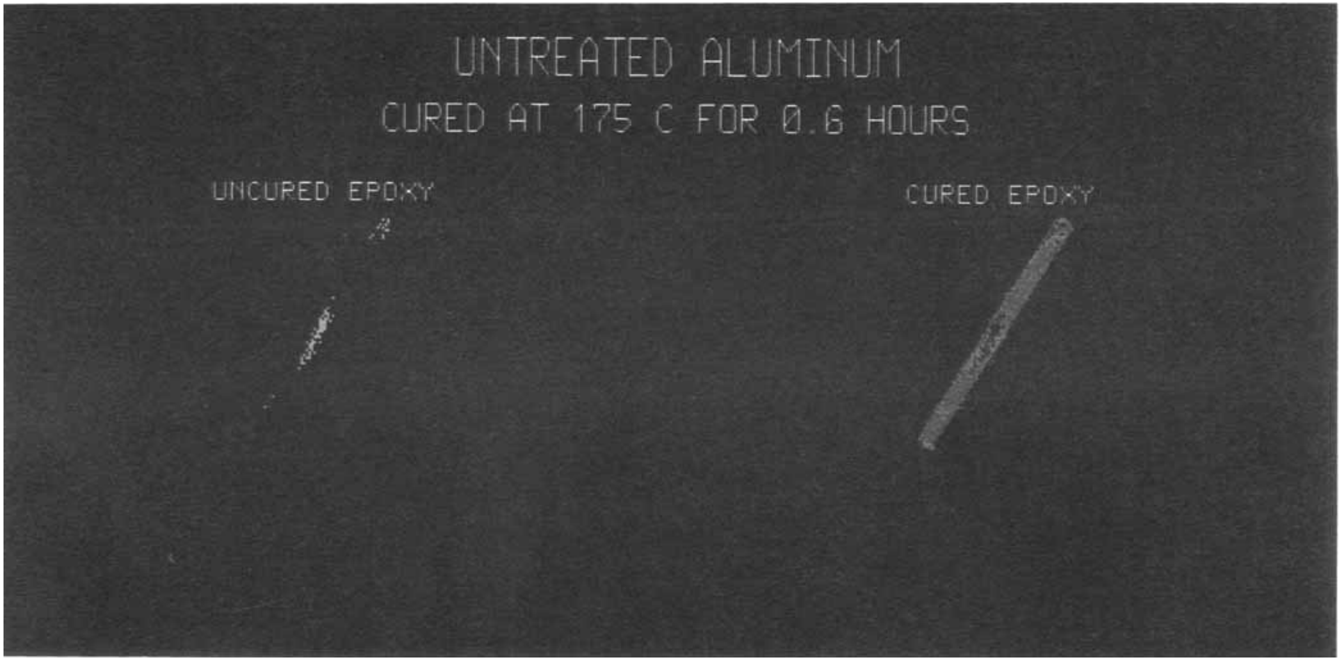

FIGURE 4 Cross-sectional NMRI images of an untreated aluminum-epoxy sample segmented into uncured and cured regions. The red area *corresponds to uncured epoxy and the green area corresponds to cured epoxy*. The image has been magnified 2.5 times. **See Color Plate III.**

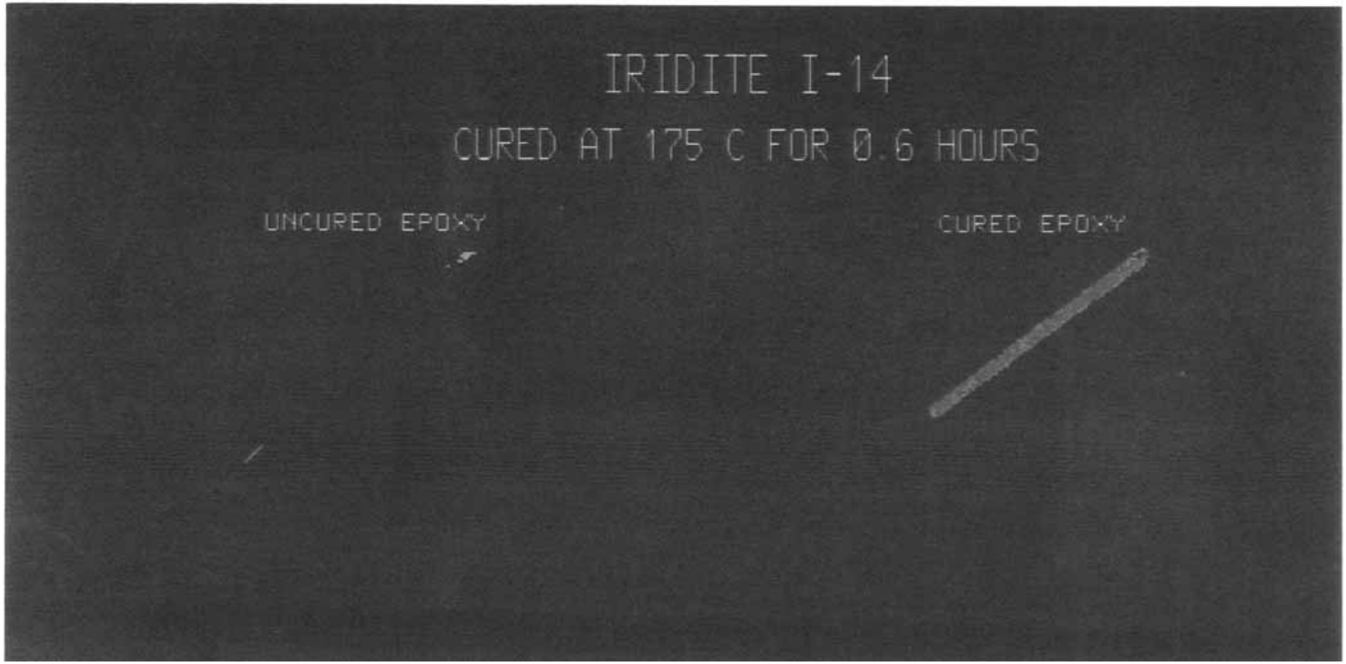

FIGURE 5 Cross-sectional NMRI images of a chemically-treated aluminum (Iridite-14®)-epoxy sample segmented into uncured and cured regions. The red area corresponds to uncured epoxy and the green corresponds to cured epoxy. The image has been magnified 2.5 times. See Color Plate IV.

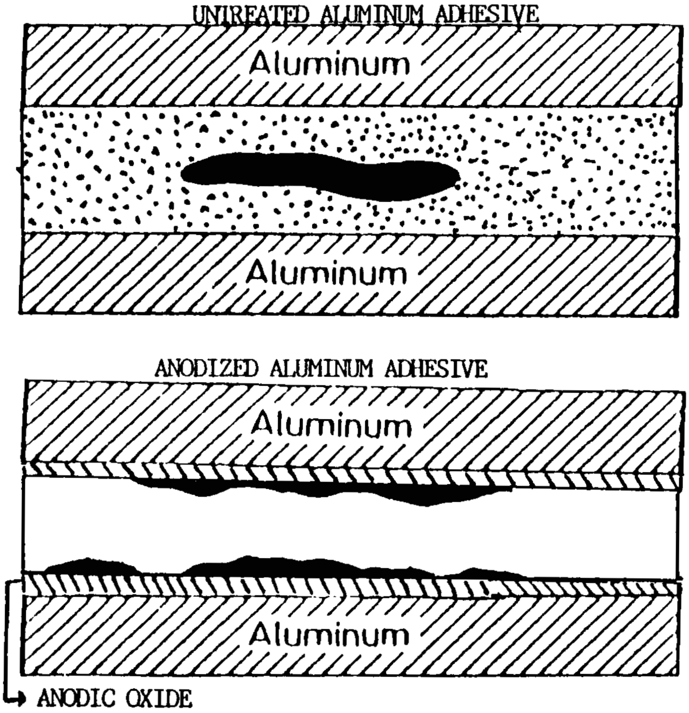

FIGURE 6 Schematic of epoxy structures in the interface region for treated and untreated samples. Dark regions are uncured regions.

Lateral NMRI Image of the Samples

Images were obtained through the bonded metal-epoxy-metal samples, thus showing a shadowgram or total projection of the samples. The NMRI images of the untreated aluminum-epoxy sample obtained at 0.2, 0.4, 0.6 and 0.8 hours of cure at 175°C are shown in Figure 7. The figures show a random distribution of the cured and uncured domains. Random distribution implies low correlation between the uncured domains. That is, there is no chemical correlation between neighbors during curing, leading to rough images. Further, there are regions, which are initially low in brightness, showing relatively high brightness at later curing times. These effects were also seen for the Iridite®-epoxy samples shown in Figure 8.

Contrasting behavior was seen for the anodized samples. As shown in Figure 9, the CAA-epoxy samples show simply connected regions for the uncured domains. The same can be said for the SAA-epoxy samples shown in Figure 10. The results can be interpreted as shown in Figure 11 where the diagrams show the expected behavior for random (left) and correlated polymerization (right).

Histogram Curve Analysis of the Lateral View NMRI Images

Histogram curves (numbers of pixels at a given cure state) were plotted for each sample as a function of cure time. Band shape analysis was performed on each curve

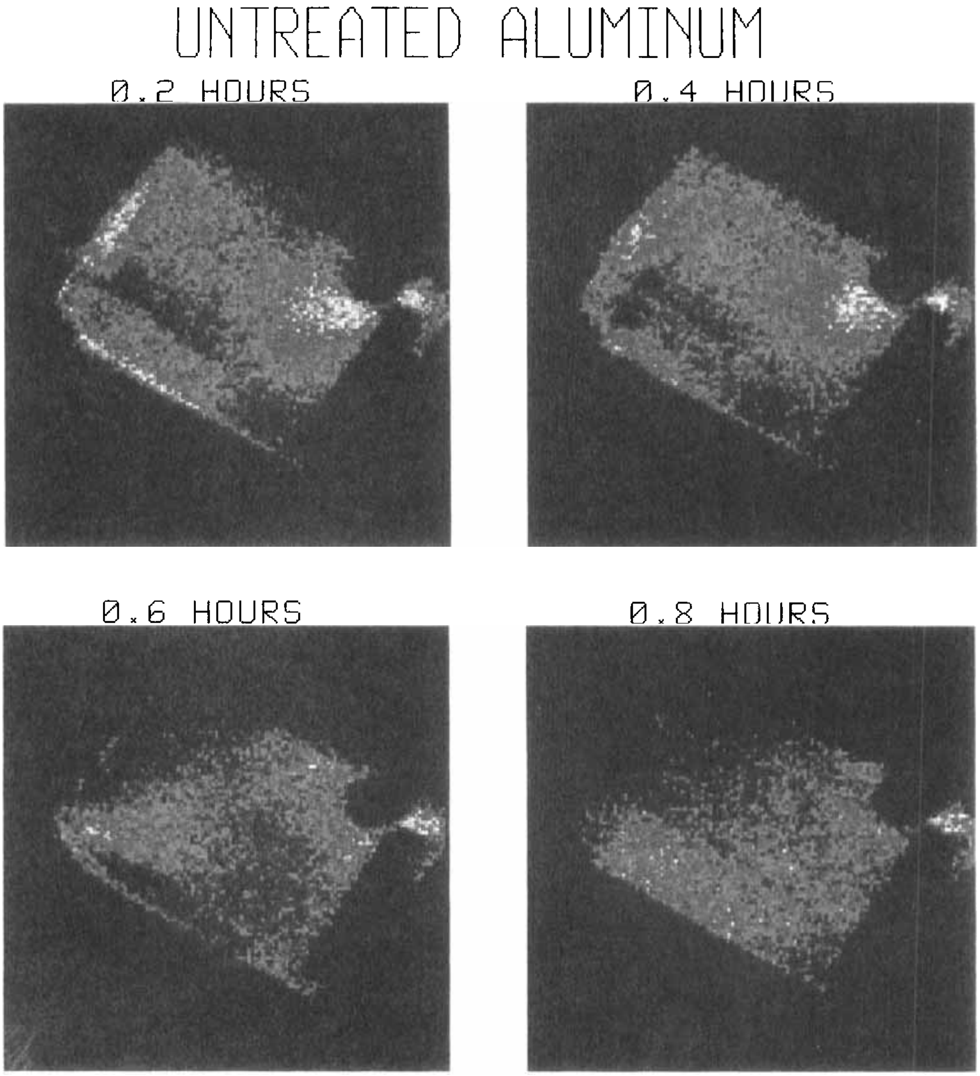

FIGURE 7 Lateral NMRI images of the untreated aluminum-epoxy sample as a function of cure time. The red domains correspond to uncured regions and the green domains correspond to cured regions. See Color Plate V.

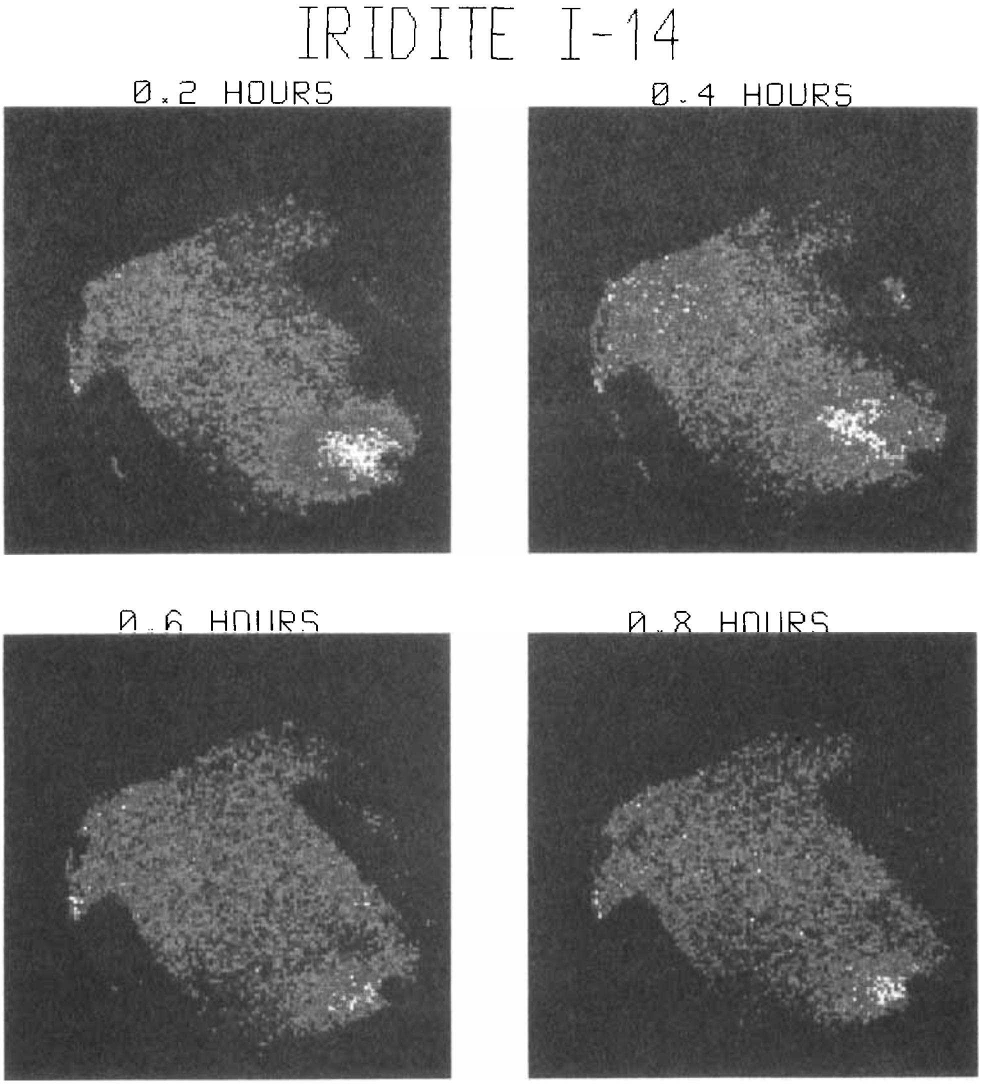

FIGURE 8 Lateral NMRI images of the chemically-treated aluminum (Iridite-14®)-epoxy sample as a function of cure time. The red regions correspond to uncured domains and the green regions correspond to cured domains. See Color Plate VI.

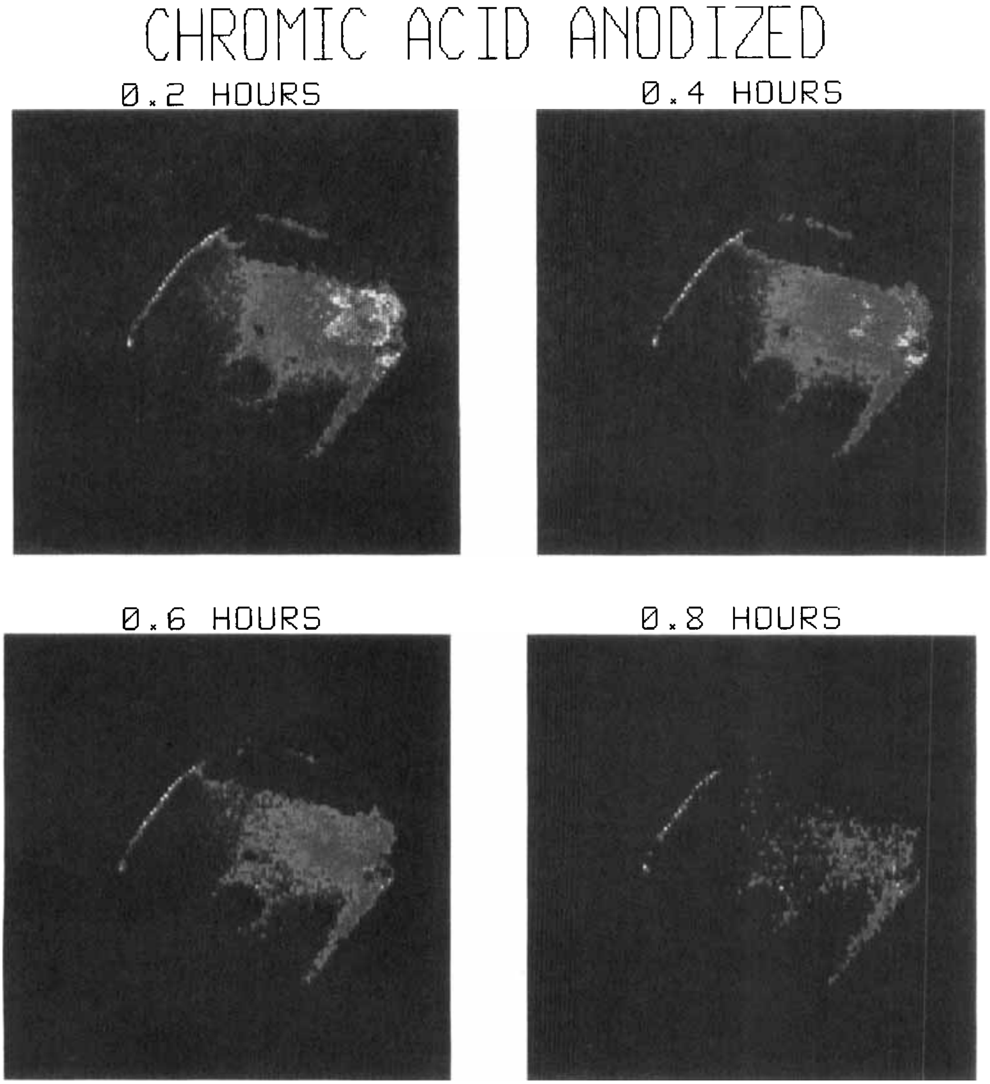

FIGURE 9 Lateral NMRI images of the CAA-epoxy sample as a function of cure time. The red regions correspond to uncured domains and the green regions correspond to cured domains.
See Color Plate VII.

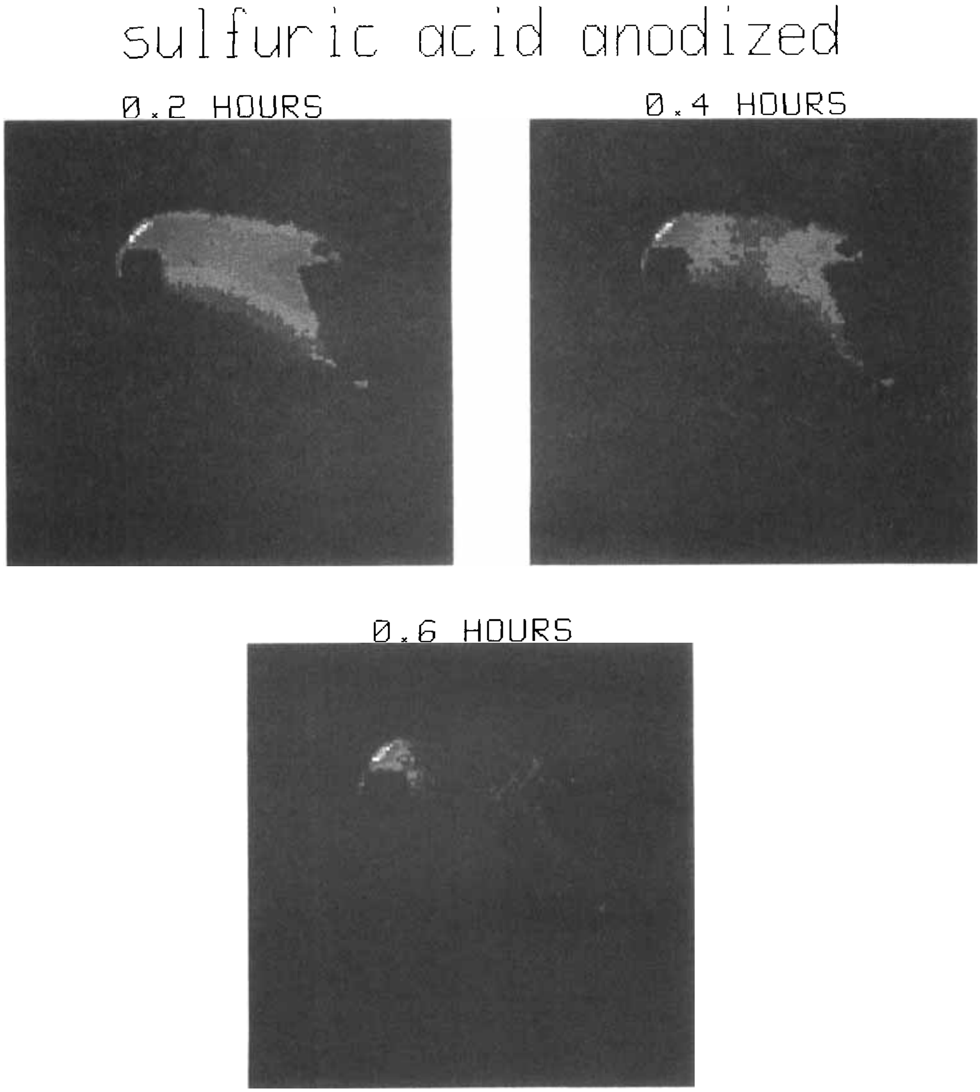

FIGURE 10 Lateral NMRI images of the SAA-epoxy sample as a function of cure time. The red regions correspond to uncured domains and the green regions correspond to cured domains. See Color Plate VIII.

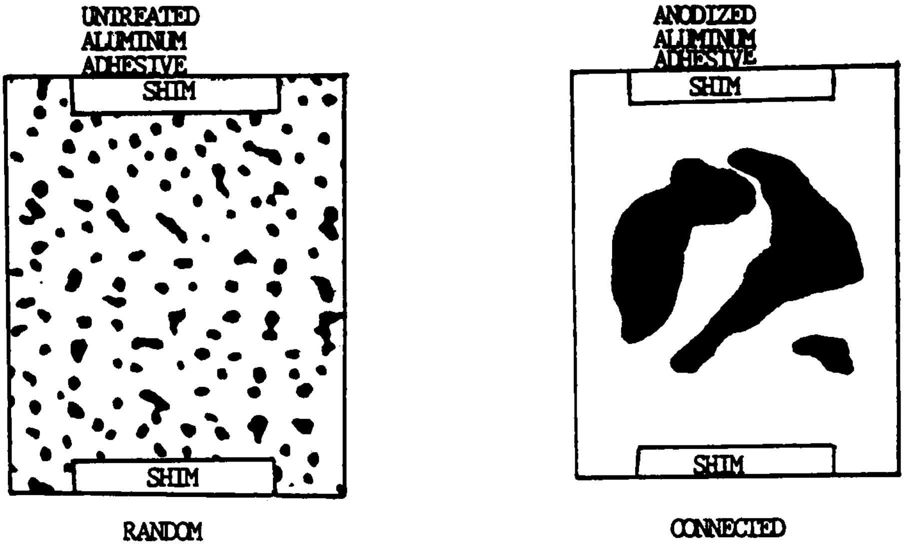

FIGURE 11 Schematic diagram of cured and uncured domains in anodized and untreated aluminum/epoxy joints. Dark regions are uncured regions.

and the results tabulated in Table II. The table shows values of the skewdness and kurtosis for each sample as a function of cure time. The skewdness is a measure of a peak's tendency to have a shoulder to the right or left of its mean. If the skewdness is positive, the peak has a shoulder to the right of its mean and if negative, the peak has a shoulder to the left of its mean. The kurtosis is a measure of how sharp a peak is. If the value is less than three, the peak is sharper than a Gaussian peak with the same width at half maximum and if greater than three is flatter than a Gaussian peak. If the kurtosis is three, then the peak is a Gaussian peak. The trend to note is the steady increase in kurtosis and skewdness values as a function of cure time for the anodized samples. Contrasting behavior is seen for the untreated and chemically-treated aluminum samples where the kurtosis as well as the skewdness goes through a minimum. These minima are due to redistribution of signal intensities within the images.

Texture Measurements

The histogram calculations are sensitive to the spatial distribution of the uncured and cured domains. To classify the images (terrain classification), gray level difference statistics[6] were performed on the images of the samples. The method is based on measuring, for a given displacement δ, the difference between the neighboring pixels at a distance δ away and the given pixel. The standard deviation calculations of the resulting difference images were obtained.

The resulting interaction between the object's distribution and size, and the sta-

TABLE II
Tabulation of the lateral view histograms

Aluminum treatment	Curing time (hours)	Mean value	Standard variation	Skewdness	Kurtosis
Untreated aluminum	0.20	69	44.7	0.83	3.38
	0.40	72	44.6	0.81	3.31
	0.60	64	37.9	0.77	3.46
	0.80	52	36.4	1.13	4.59
	1.00	58	36.0	0.81	3.85
	1.20	35	30.0	2.00	—
Iridite® treated aluminum	0.20	60	37.1	1.25	5.05
	0.40	58	36.4	1.27	5.09
	0.60	58	33.2	0.68	3.72
	0.80	42	25.7	0.90	4.05
	1.00	28	19.6	1.06	—
	1.20	34	27.5	1.32	5.23
SAA anodized aluminum	0.20	58	32.9	0.29	3.62
	0.40	46	27.4	1.22	7.61
	0.60	25	27.9	3.52	—
CAA anodized aluminum	0.20	71	50.1	0.53	2.30
	0.40	69	45.8	0.44	2.43
	0.60	54	34.8	0.79	4.07
	0.80	43	34.1	1.51	6.26

tistical window (the size of the neighborhood) can be seen in Figure 12. The figure shows a plot of the gray level difference standard deviation and the neighborhood's size for the untreated and CAA-treated aluminum samples.

The untreated aluminum sample is characterized by an initial rise, characteristic of very rough images, and then the standard deviation reaches a steady value at a pixel neighborhood of 140 μm. The appearance of this plateau indicates a uniform distribution of objects inside the statistical window, that is, any neighborhood size bigger than 140 μm has a uniform distribution of domain size.

In contrast, the anodized samples are characterized by a very low and constant standard deviation value. This is characteristic of very coarse images where constant brightness values in large domains gives low deviations.

In order to see the effect of the surface treatment on the spatial distribution of cured and uncured domains during the curing process, the standard deviation from a neighborhood of fixed size (84 μm) was measured as a function of curing time for the treated and untreated aluminum-epoxy samples. The images of the sulfuric acid anodized-epoxy samples are characterized by a constant standard deviation in the early stages of cure, and then the standard deviation value rises at the end of the cure reflecting the low NMR signal (see Figure 13).

The images of the untreated aluminum-epoxy samples are characterized by a rise in the standard deviation in the early curing process (see Figure 13) reflecting a domain redistribution effect. The rise in standard deviation value is probably due to dispersion of low molecular material within the sample. This phenomenon was also seen in the chemically-treated aluminum-epoxy samples (see Figure 14).

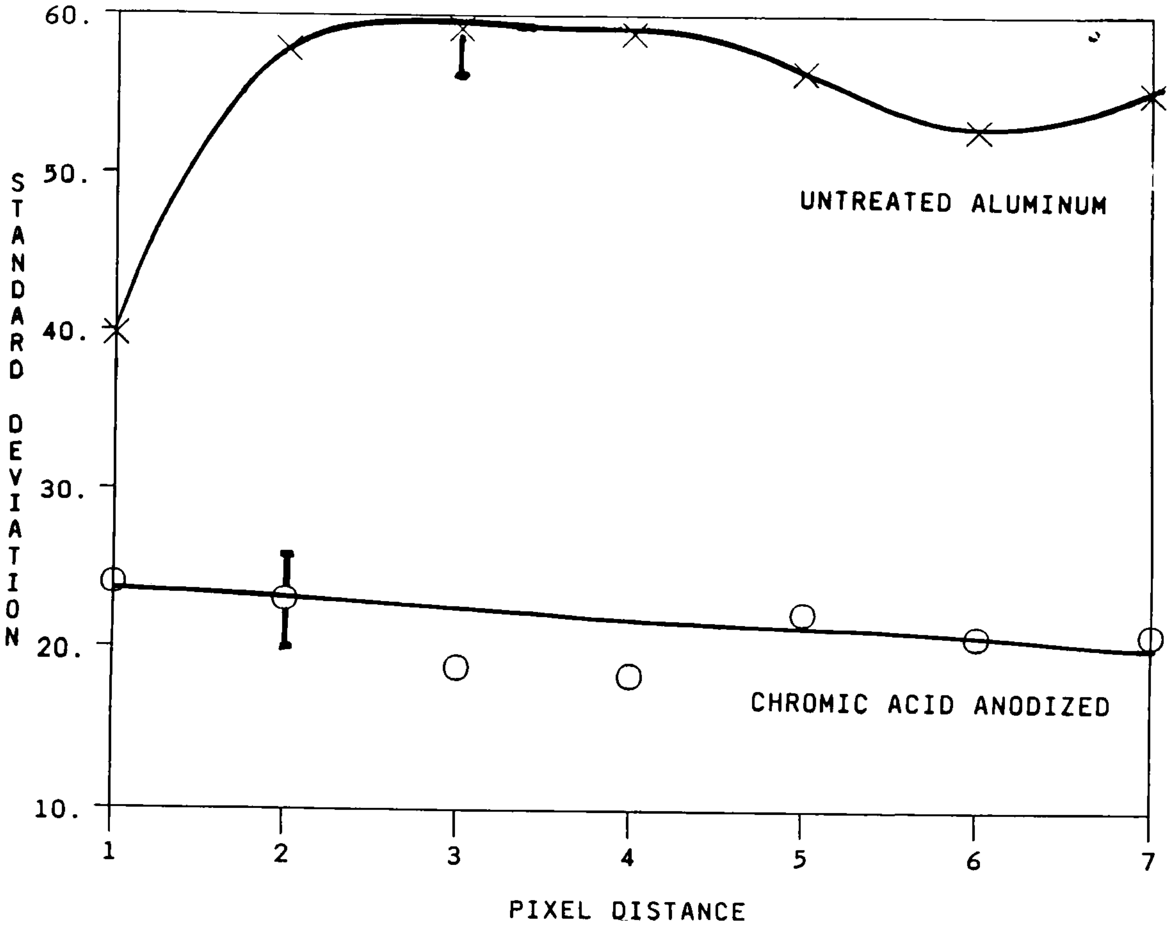

FIGURE 12 Standard deviation values from different statistics as a function of neighborhood size (number of pixels away from given pixel) for the untreated aluminum and CAA-epoxy samples.

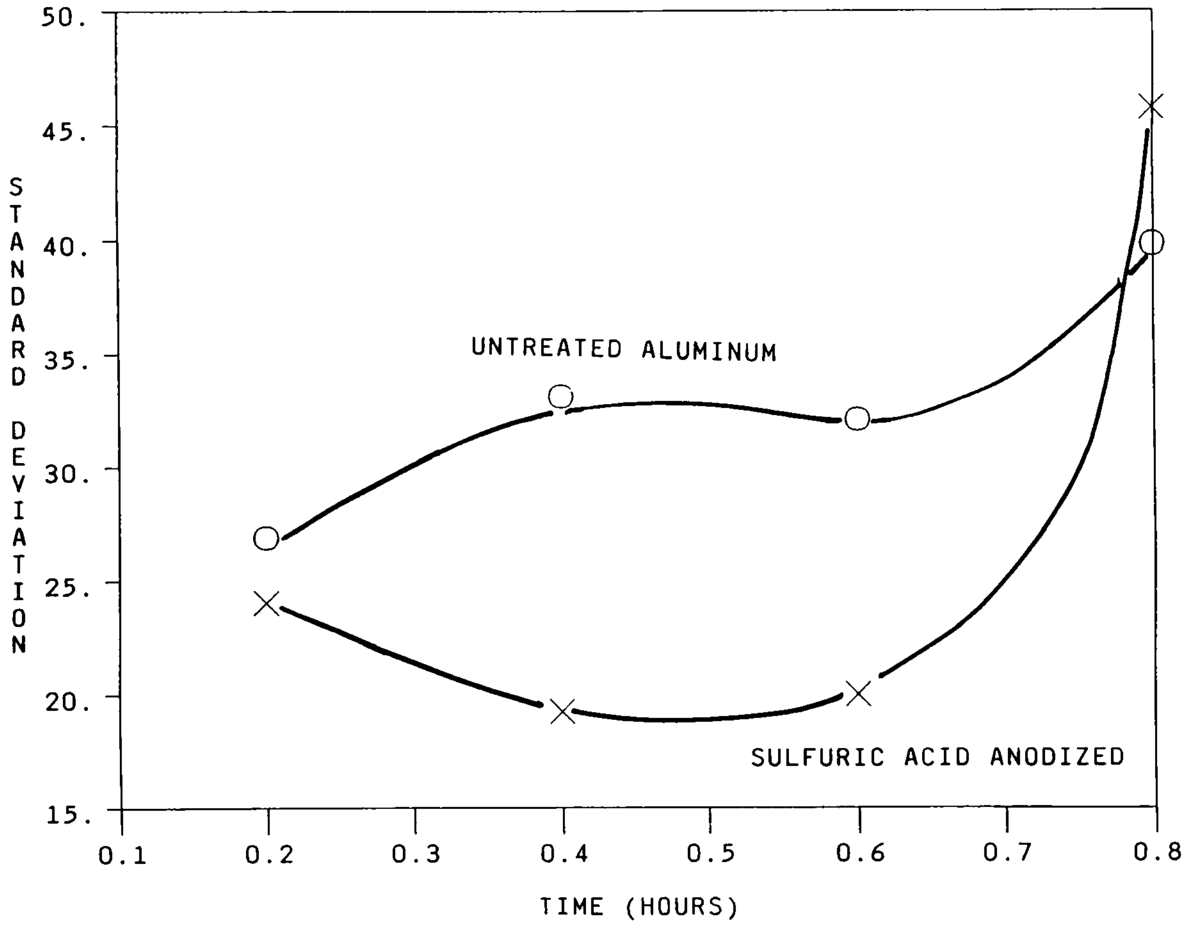

FIGURE 13 Standard deviation values from different statistics with a 3 × 3 pixel window as a function of cure time for the untreated aluminum and SAA-epoxy samples.

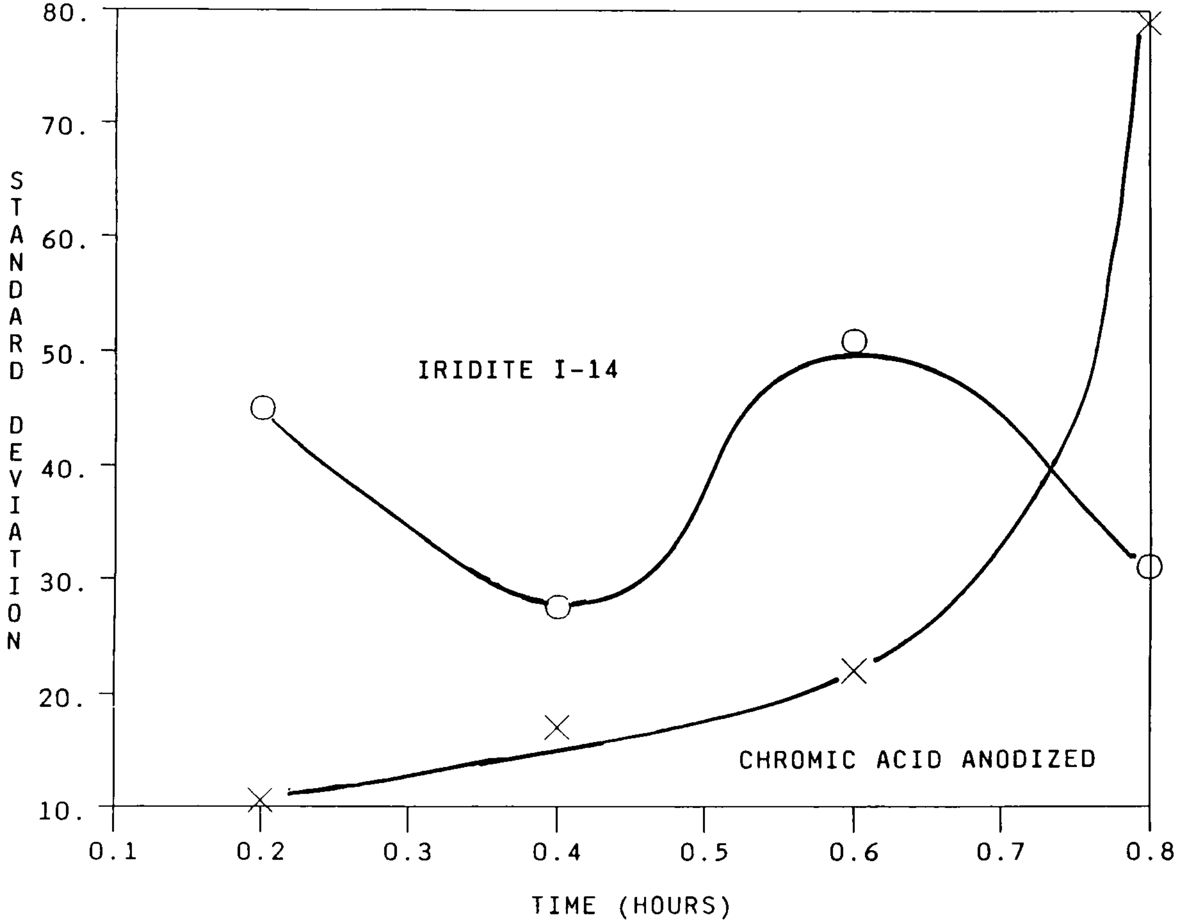

FIGURE 14 Standard deviation values from different statistics with a 3 × 3 pixel window as a function of cure time for the chemically treated aluminum (Iridite) and CAA-epoxy samples.

CONCLUSIONS

Image analysis of NMRI pictures was used to analyze the epoxy curing process in the presence of chemically-treated aluminum surfaces. The curing process was slower on the untreated and chemically-treated aluminum surfaces than on the anodized aluminum surfaces. This was probably due to the dispersion of low molecular weight material. There was no dispersion detected in the epoxy cured in contact with anodized aluminum samples. The images in the untreated as well as in the chemically-treated aluminum samples showed high texture, indicative of a Gaussian image. That is, the high mobility domains were not connected in the images. In the case of the anodized surfaces, the high mobility domains were simply connected, showing little texture, and this was attributed to interactions between the epoxy and the anodized surface. Our previous work has shown that the epoxy preferentially segregates to the anodized surface and this effect might be occurring here.[9] A theory of the curing of the epoxy has assumed that mobility plays a role in the curing process, especially at the late stages. For the anodized samples, the curing process is best analyzed and modelled by assuming no mobility but, rather, caging effects.

References

1. C. Macoski and D. Miller, *Macromolecules* **3** (2), 199 (1976).
2. F. J. Boerio and P. P. Hong, *Ind. & Eng. Chem.* **A126,** 245 (1990).
3. R. O. Carter III, C. A. Gerczak and R. A. Dickie, *Appl. Spectros.* **4** (5), 649 (1986).
4. D. J. Ondrus and F. J. Boerio, *J. Adhesion* **29,** 27 (1989).
5. A. O. K. Nieminen and J. L. Koenig, *J. Adh. Sci. Technol.* **2,** 407 (1988).
6. J. S. Wezka, C. R. Dyer and A. Rosenfield, *IEEE Trans. on System, Man. and Cybern.* **SMC-6** (4), 269 (1976).
7. H. Y. Carr and E. M. Purcell, *Phys. Rev.* **94,** 630 (1954).
8. S. Meiboom and D. Gill, *Rev. Sci. Instrum.* **29,** 688 (1958).
9. F. Fondeur and J. L. Koenig, *Appl. Spectroscopy* **47,** 1 (1993).
10. A. O. K. Nieminen and J. L. Koenig, *J. Adhesion* **30,** 47 (1989).